# Raman Scattering Study of High-Pressure Phase Transition in Thiourea

**Ankita Banerji and S. K. Deb***

*High Pressure Physics Division, Bhabha Atomic Research Center, Mumbai 400085, India*

*Received: April 3, 2007; In Final Form: July 4, 2007*

A high-pressure Raman spectroscopic study of phase transitions in thiourea is reported. The changes in the Raman spectra with increasing and decreasing pressure have been followed to a maximum pressure of ≈11GPa. We observe several changes in the spectra including splitting of modes, appearance of new modes, and sudden change in the slope of the frequency−pressure curve at several pressures. On the basis of this study, we propose the existence of three more transitions in this system to phases VII, VIII, and IX at ≈1, 3, and 6.1 GPa, respectively, in addition to the V−VI phase transition at 0.35 GPa reported earlier. All the transitions have been found to be completely reversible. We interpret these changes in terms of symmetry-lowering phase transitions.

## 1. Introduction

Thiourea ($NH_2-CS-NH_2$) is a simple organic molecular crystal and has been the subject of several structural studies at ambient as well as low-temperature and high-pressure conditions.[1−3] Its molecular formula and structure are similar to those of urea with the O atom in urea replaced by S. It is ferroelectric below 169 K, and its ferroelectric behavior is associated with the rotational and translational displacements of the molecules within the crystal.[4] It goes to the paraelectric phase above 202 K through an intermediate incommensurate phase.[5] Apart from being a molecular ferroelectric crystal, it finds application as an efficient inhibitor to prevent corrosion of iron in acidic media due to chemisorption on the surface, and it is also used for the evolution of $H_2$ at the surface of Hg.[6,7] It also acts as a catalyst for accelerating electroreduction of cations like $Zn^{2+}$ and $Cd^{2+}$.[8] Like urea, it is also a planar molecule with $C_{2v}$ symmetry and at ambient conditions it crystallizes in orthorhombic *Pbnm*, $Z = 4$ (Phase V), unlike urea which crystallizes in tetragonal $P42_1m$ ($Z = 2$) space group.[9] The molecules lie with the C and S atoms in the mirror planes at $y = 1/4$ and 3/4 with two equivalent $NH_2$ groups on either side of it. The thiourea molecules in the crystal interact via N−H···S hydrogen bonding. The planar thiourea molecules are arranged as "ribbons" which are linked along the *c*-axis in a head-to-tail fashion, and each sulfur atom participates in four hydrogen bonds.[10]

Extensive structural measurements on this material have been made using X-ray and neutron diffraction and also using spectroscopic techniques in its paraelectric and ferroelectric phases.[11−13] However, pressure-dependent investigations on this material have been very limited. Bridgman[14] revealed a high-pressure transition to phase VI by using volumetric techniques, and Figuiere et al.[15] reported a detailed pressure−temperature phase diagram study of thiourea probing the low-frequency Raman modes. Phase VI has also been investigated by Leonidova[16] using electric polarization and capacitance measurements and by Kabalkina[17] using XRD. All these studies indicated that thiourea undergoes a transition to a high-pressure phase at 0.35 GPa. The structure of the high-pressure phase VI has been determined and has the same space group with $Z = 12$ and cell tripling along the *c*-axis with condensation of the $\Lambda_4$ mode with $k = c^*/3$. However the lattice constants *a* and *b* remain practically the same and the transition is first-order, with 5% volume reduction across the transition. The deformation of molecules through the V−VI transition is small, and deviation of positions of S, C, and N atoms with respect to the molecule is negligible. The transition involves rotation and translation of the molecules and also changes the hydrogen-bonding network connecting the molecules along the *c*-axis and between molecules related by *b*-glide plane symmetry operations.[18] However, there has been no other high-pressure investigation on thiourea, and its high-pressure structure other than the phase VI structure is not known.

It is worth noting here that the related higher-symmetry compound urea ($NH_2-CO-NH_2$) also shows interesting behavior at high pressures. At ambient conditions, urea exists in a tetragonal structure $P42_1m$ and consists of ribbons of molecules linked in a head-to-tail fashion along the tetragonal *c*-axis. In particular, the hydrogen bond N−H···O in urea has been found to play an important role in inducing high-pressure phase transitions. The high-pressure behavior of urea has been investigated with the help of Raman spectroscopy up to a pressure of 15 GPa.[19,20] A symmetry-lowering phase transition (tetragonal → orthorhombic) at 0.6 GPa was confirmed, and another subtle phase transition associated with the appearance of new modes and discontinuous change in slopes at 9 GPa was reported.[19] In particular, the asymmetric stretch $NH_2$ mode shows a gradual decrease till 0.6 GPa where it shows an abrupt increase in frequency and then continuously decreases. This clearly indicates an increase of hydrogen bonding in the parent phase and decrease at the phase transition at 0.6 GPa.[19] A more recent detailed high-pressure Raman scattering and X-ray diffraction study in urea by Lamelas et al.[20] has shown clearly the existence of three high-pressure transitions at 0.5, 5, and 8 GPa. Their micro-Raman study has revealed the existence of two different domains in the two higher-pressure phases. Although the hydrogen bonding through N−H···S plays a significant role in the crystal structure of thiourea, the final structure and high-pressure phase transitions are quite different from those in urea. Thus, a high-pressure study of thiourea and

* Corresponding author. Phone: +91-22-25595038. Fax: +91-22-25505151/25519613. E-mail: sudip51@gmail.com.

10.1021/jp072604w CCC: $37.00 
Published on Web 08/28/2007

**TABLE 1: Vibrational Frequencies of Lattice Modes and Their Pressure Derivatives in Phases V, VI, VII, VIII, and IX**

| phase V | | | | phase VI | | phase VII | | phase VIII | | phase IX | |
|---|---|---|---|---|---|---|---|---|---|---|---|
| frequency ($\omega$), cm$^{-1}$ | mode vibration | symmetry | slope (d$\omega$/d$P$) | frequency ($\omega$), cm$^{-1}$ | slope (d$\omega$/d$P$) | frequency ($\omega$), cm$^{-1}$ | slope (d$\omega$/d$P$) | frequency ($\omega$), cm$^{-1}$ | slope (d$\omega$/d$P$) | frequency ($\omega$), cm$^{-1}$ | slope (d$\omega$/d$P$) |
| 45.9 ± 0.1 | lattice mode | | 17.5 | 56.4 ± 0.04 | 0.36 | 56.8 ± 0.03 | 4.67 ± 0.4 | 67.9 ± 0.03 | 1.87 ± 0.2 | 74.8 ± 0.03 | 1.3 ± 0.04 |
| | | | | | | 62.4 ± 0.1 | −1.7 ± 0.02 | | | | |
| 63.6 ± 0.04 | lattice mode | | 10.5 | | | | | | | | |
| | | | | 78.9 ± 0.5 | 15.5 | 85 ± 0.3 | 4.4 ± 0.07 | 95.1 ± 0.3 | 4.45 ± 0.2 | 107.6 ± 0.2 | 1.8 ± 0.4 |
| | | | | 86.2 ± 0.6 | 30.5 | 100.1 ± 0.2 | 5.1 ± 0.3 | 113.9 ± 0.6 | 5 ± 0.3 | 124.3 ± 0.8 | −0.46 ± 0.1 |
| | | | | | | | | | | 166.5 ± 0.1 | −1.5 ± 0.1 |
| 102 ± 0.1 | lattice mode | | 41.5 | 118.6 ± 0.1 | 35.9 | 141 ± 0.2 | 4.44 ± 0.9 | 154.6 ± 0.2 | 12.59 ± 1.4 | 180.9 ± 0.2 | −1.04 ± 0.2 |
| 119 ± 0.2 | lattice mode | | 47.5 | 138 ± 0.2 | 30.3 | 156.2 ± 0.3 | 5.84 ± 0.9 | 173 ± 0.5 | 8.38 ± 0.7 | 194 ± 0.3 | −0.74 ± 1.1 |

**TABLE 2: Vibrational Frequencies of Modes Lying between 300 and 1200 cm$^{-1}$ and Their Pressure Derivatives in Phases V, VI, VII, VIII, and IX**

| phase V | | | | phase VI | | phase VII | | phase VIII | | phase IX | |
|---|---|---|---|---|---|---|---|---|---|---|---|
| frequency ($\omega$), cm$^{-1}$ | mode vibration | sym-metry | slope (d$\omega$/d$P$) | frequency ($\omega$), cm$^{-1}$ | slope (d$\omega$/d$P$) | frequency ($\omega$), cm$^{-1}$ | slope (d$\omega$/d$P$) | frequency ($\omega$), cm$^{-1}$ | slope (d$\omega$/d$P$) | frequency ($\omega$), cm$^{-1}$ | slope (d$\omega$/d$P$) |
| 401 ± 0.1 | NCS deform | $B_{1g}$ | 13.5 | 406.4 ± 0.2 | 5.68 ± 1 | 409.3 ± 0.1 | 3.2 ± 1.46 | 415.3 ± 0.1 | 2.2 ± 0.2 | | |
| | | | | 375.4 ± 0.4 | −2.97 ± 3.2 | 373.3 ± 0.3 | −5 | 362.8 ± 0.2 | −5.43 ± 0.3 | | |
| | | | | | | | | 368.9 ± 0.2 | 2.62 ± 0.4 | | |
| | | | | 396.8 ± 0.5 | 2.5 ± 2.6 | 398.3 ± 0.5 | 2 ± 1.6 | 408.5 ± 0.3 | 0.76 ± 0.2 | 410.2 ± 0.2 | 0.63 ± 0.3 |
| | | | | | | | | 472.4 ± 0.2 | −0.35 ± 0.1 | 471.3 ± 0.1 | 0.48 ± 0.3 |
| 477.8 ± 0.06 | CN deform | $A_g$ | −13 | 472.6 ± 0.1 | 3.57 ± 1.9 | 473.9 ± 0.1 | 1.43 ± 1.4 | 479.1 ± 0.2 | 2.09 ± 0.1 | 486.4 ± 0.1 | 1.24 ± 0.1 |
| | | | | | | | | | | 515.9 ± 0.4 | −0.38 ± 0.7 |
| 499.6 ± 0.4 | $NH_2$ twist | $A_g$ | −10.5 | 495.4 ± 0.3 | 12.13 ± 0.6 | 501.7 ± 0.2 | 5.61 ± 0.9 | 511.7 ± 0.1 | 3.91 ± 0.1 | 533.9 ± 0.3 | 0.99 ± 0.2 |
| 572 ± 0.4 | $NH_2$ twist | $B_{2g}$ | 13.5 | 577.4 ± 0.4 | −4.2 ± 1.8 | 574.2 ± 0.4 | −0.53 ± 0.3 | | | | |
| 620.3 ± 0.5 | SCNN torsion | $A_g$ | −25.7 | 610 ± 0.5 | −2.65 ± 1.2 | 606.3 ± 0.5 | −0.32 ± 0.2 | 608.3 ± 0.5 | −1.32 ± 0.4 | | |
| | | | | | | | | | | 605.7 ± 0.4 | 0.77 ± 0.2 |
| | | | | | | | | | | 636 ± 0.5 | 2.68 ± 0.2 |
| 655 ± 0.5 | SCNN torsion | $B_{2g}$ | −44 | 637.4 ± 0.5 | 4.78 ± 0.1 | 639.8 ± 0.5 | 1.45 ± 0.1 | | | | |
| | | | | 652.9 ± 0.4 | 5.92 ± 1 | 657.6 ± 0.5 | 1.22 | 661.3 ± 0.4 | 2.36 ± 0.3 | | |
| | | | | | | | | | | 713.5 ± 0.7 | 2.86 ± 0.1 |
| 732.8 ± 0.03 | $SCN_2H_4$ stretch | $A_g$ | 0 | 728.2 ± 0.03 | 6.76 ± 2 | 731.4 ± 0.03 | 4.08 ± 1.3 | 738.8 ± 0.05 | 3.32 ± 0.3 | 749.7 ± 0.09 | 0.38 ± 0.5 |
| | | | | 740.3 ± 0.1 | 12.1 ± 0.8 | 738.3 ± 0.1 | 5.61 ± 0.9 | 756.2 ± 0.1 | 3.28 ± 0.5 | 765.6 ± 0.08 | 1.91 ± 0.1 |
| | | | | 1087.3 ± 0.4 | 6.66 ± 1.2 | 1090.7 ± 0.4 | 3.54 ± 1.5 | 1096.2 ± 0.3 | 2.43 ± 0.3 | 1104.4 ± 0.1 | 1.8 ± 0.3 |
| 1093.2 ± 0.05 | $SCN_2H_4$ stretch | $A_g$ | 1.5 | 1096.2 ± 0.1 | 8.87 ± 1.1 | 1100.7 ± 0.1 | 5.5 ± 1 | 1110 ± 0.07 | 3.71 ± 0.3 | 1120 ± 0.04 | 2.06 ± 0.4 |

**TABLE 3: Vibrational Frequencies of Modes between 3000 and 3500 cm$^{-1}$ and Their Pressure Derivatives in Phases V, VI, VII, VIII, and IX**

| phase V | | | | phase VI | | phase VII | | phase VIII | | phase IX | |
|---|---|---|---|---|---|---|---|---|---|---|---|
| frequency ($\omega$), cm$^{-1}$ | mode vibration | sym-metry | slope (d$\omega$/d$P$) | frequency ($\omega$), cm$^{-1}$ | slope (d$\omega$/d$P$) | frequency ($\omega$), cm$^{-1}$ | slope (d$\omega$/d$P$) | frequency ($\omega$), cm$^{-1}$ | slope (d$\omega$/d$P$) | frequency ($\omega$), cm$^{-1}$ | slope (d$\omega$/d$P$) |
| 3177.5 ± 0.1 | $NH_2$ stretch (sym) | $A_g$ | −30.2 | 3165.4 ± 0.2 | −2.87 ± 0.6 | 3163.3 ± 0.3 | −8.51 ± 1 | 3154.8 ± 0.1 | −4.71 ± 0.1 | 3138 ± 0.2 | −5.9 ± 1.1 |
| | | | | 3182.8 ± 0.3 | −4.76 ± 1.4 | 3180.4 ± 0.4 | −17.7 ± 3.4 | | | | |
| | | | | 3213.8 ± 0.3 | −3.63 ± 0.3 | 3211.9 ± 0.4 | −1.97 ± 0.5 | | | | |
| | | | | | | | | 3217.4 ± 0.4 | 2.03 ± 0.3 | 3225.1 ± 0.8 | |
| 3231.8 ± 0.5 | NH stretch | $B_{1g}$ | −13 | | | | | | | | |
| | | | | 3238.3 ± 0.6 | 2.66 ± 0.5 | 3236.3 ± 0.6 | −2.04 ± 0.6 | | | | |
| 3281.4 ± 0.2 | NH stretch | $A_g$ | −13.7 | 3275.9 ± 0.08 | −2.82 ± 0.1 | 3273.6 ± 0.1 | −3.28 ± 0.8 | 3268.2 ± 0.3 | −0.4 ± 0.2 | 3265 ± 0.6 | |
| 3308.8 ± 1.5 | nnot listed | | −25 | | | | | | | | |
| | | | | 3339.8 ± 0.5 | −11.4 | 3337.8 ± 0.6 | −8.36 ± 0.4 | | | | |
| 3371.8 ± 0.05 | $NH_2$ stretch (asym) | $A_g$ | 12.7 | 3376.9 ± 0.05 | −12 | 3369 ± 0.03 | −8.06 ± 0.8 | 3357 ± 0.08 | −3.5 ± 0.4 | 3348 ± 0.08 | 0.2 ± 0.6 |

its comparison with those for urea will provide important differences in the role of hydrogen bonding in these two systems as regards their structure across the high-pressure phase transitions.

In this paper, we present results of our Raman scattering measurements on the thiourea up to a pressure of ≈11 GPa. Since the molecules are bonded through hydrogen-bonding N−H···S, it is expected that the strength of the hydrogen bonding will undergo considerable changes with increasing pressure, which in turn will play an important role in any high-pressure transition.

## 2. Experimental Details

The high-pressure experiments were carried out on polycrystalline thiourea samples loaded in a Diacel Products DAC (model B-05) with 600 $\mu$m culet. The sample was loaded in a 200 $\mu$m hole drilled in a 250 $\mu$m thick SS 301 gasket pre-indented to 70 $\mu$m thickness. The pressure calibration was done using ruby fluorescence. No pressure-transmitting liquid medium was used in the experiment because most of the conventional organic pressure-transmitting fluids have been found to dissolve thiourea. We have monitored the separation between the $R_1$ and $R_2$ components of the ruby fluorescence line which has been found to remain invariant even at the highest pressure, indicating a negligible nonhydrostatic component.[21] In addition, thiourea is quite soft (bulk modulous ≈ 8 GPa), and hence the pressure can be considered to be quasihydrostatic (if not exactly hydrostatic) even at the highest pressure. The Raman spectra were excited using the 514.5 nm line from an $Ar^+$ laser and also the 532 nm line from a solid-state laser. The

scattered light over the range 30−200 $cm^{-1}$ was analyzed using a double monochromator with cooled GaAs PMT, and for photon counting for the range >200 $cm^{-1}$ we have used a single-stage 0.9 m spectrograph (with notch filter) and back-thinned CCD detector. Spectra were also recorded while reducing the pressure.

### 3. Results and Discussion

The point group symmetry of the thiourea molecule is $C_{2v}$, and they occupy $C_s$ sites in the ambient-pressure unit cell with factor group $D_{2h}$. Group theoretical classification of the normal vibrations allows 93 optical modes, and the Raman active modes are distributed as 12 lattice modes belonging to $3A_g + 3B_{1g} + 3B_{2g} + 3B_{3g}$ symmetry. The rest of them are internal modes distributed as $10A_g + 10B_{1g} + 8B_{2g} + 8B_{3g}$. The ambient Raman spectrum and the different mode frequencies agree quite well with the values reported in the literature.[21] However, all the allowed modes could not be observed, and this may be due to very small splitting between the correlation components and very weak intensities of many modes. As a polarization-dependent study from single crystals was not available, the mode assignment was done with the help of the reported lattice dynamical calculation and other Raman and IR spectra.[23,24] Tables1−3 give the vibrational frequencies of the observed Raman modes with their assignments and their pressure derivatives in different phases. In these tables we have also included any new mode appearing in any phase with the corresponding slopes. The errors in the corresponding quantities are also included. However, we would like to mention here that phase V has only two data points and it was not meaningful to extract any errors in the slope, and hence have not been shown in the tables. The nature of these new modes can be obtained by correlating their origin to the corresponding mode in the ambient phase. These tables can be used to calculate the frequencies of different modes at pressure $P$ in any particular phase from the following relation:

$$\omega(P) = \omega(P_0) + (P - P_0)\left(\frac{\partial\omega}{\partial P}\right) \quad (1)$$

where $\omega(P_0)$ and $(\partial\omega/\partial P)$ are the frequency and slope values listed in the tables, and $P_0$ is lowest value of the pressure in that phase.

Figure 1 shows the changes in the Raman spectra with increasing pressure over the range covering the low-frequency lattice vibration modes representing translation and libration modes. Figure 2 shows the spectral changes with increasing pressure over the range covering the several skeletal and internal modes and the higher-frequency range. The modes with frequencies more than 3000 $cm^{-1}$ arise solely from N−H stretching vibrations, whereas those between 400 and 1700 $cm^{-1}$ arise due to bending, twist, and deformation modes and are usually of mixed character. Lower values of the N−H stretching vibrations in the solid compared with those from the solution spectra are mainly due to the presence of N−H···S hydrogen bonding. The ambient spectra over 3000−3500 $cm^{-1}$ could be resolved into five bands, and the two most intense bands at 3181 and 3375 $cm^{-1}$ could be identified as $A_g$ symmetric and antisymmetric $N-H_2$ stretch modes. Although the mode at 3284 $cm^{-1}$ matches one of the Fermi resonance (FR) components,[26] the other two modes at 3235 and 3305 $cm^{-1}$ do not match any other known frequencies and so it is difficult to interpret their origin.

**Phase V−VI.** As the pressure is slowly increased, we observe considerable changes in the spectrum such as splitting of the existing modes and appearance of new modes together with changes in the intensity distribution of various modes over the whole spectral range. It can be seen from Figure 1 that there is a sudden and considerable change in the intensity distribution of the two lowest-frequency lattice modes at 46 and 63 $cm^{-1}$ across the V−VI transition at ≈0.4 GPa and in phase VI there exists only one mode with frequency ≈57 $cm^{-1}$; our observation

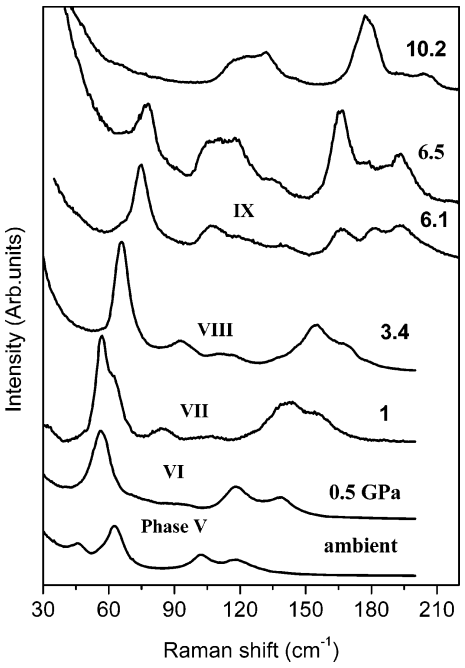


**Figure 1.** Raman spectra of thiourea over 20−220 $cm^{-1}$ representing lattice vibration modes with increasing pressure (GPa).

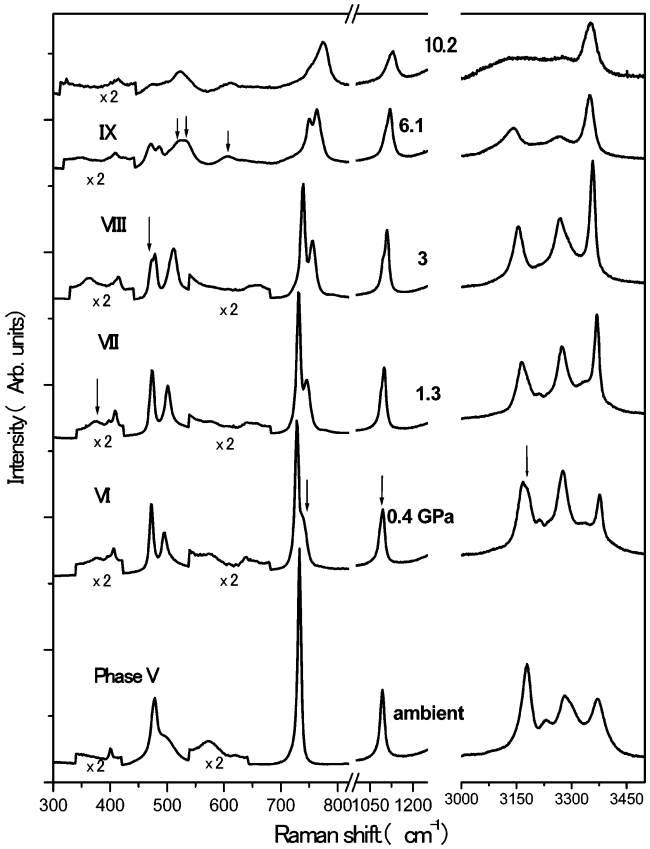


**Figure 2.** Raman spectra of thiourea over 400−1700 $cm^{-1}$ corresponding to skeletal and internal modes of vibrations and over 3000−3500 $cm^{-1}$ corresponding to NH stretching vibrations.

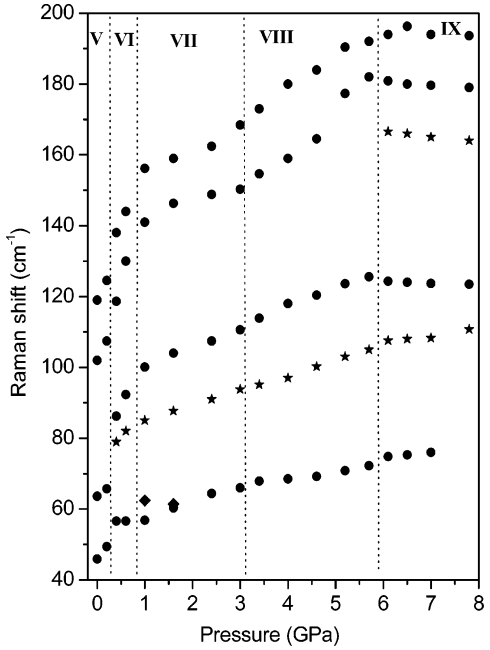


**Figure 3.** Change in frequency of vibrational modes of thiourea over 20−220 cm$^{-1}$ as a function of pressure.

agrees quite well with the results reported earlier.[25] The variation in frequency of low-frequency modes with increasing pressure is shown in Figure 3, and it can be seen that the 46 cm$^{-1}$ mode increases at the rate of ≈17 cm$^{-1}$/GPa till 0.4 GPa and then reduces to 0.4 cm$^{-1}$/GPa as listed in Table 1. We also observe several changes in the spectra corresponding to the modes belonging to the internal vibrations as shown in Figure 2. There is a gradual change in the intensity of the modes at 478 and 500 cm$^{-1}$ accompanied by a sudden narrowing in phase VI. The FWHM for these modes decreases from 14 and 30 cm$^{-1}$ to 7 and 13 cm$^{-1}$, respectively, across the V−VI transition. In addition, we observe the appearance of several new modes; for example, there are two modes near the low-frequency side of the 401 cm$^{-1}$ mode, one mode on the higher-frequency side of the $NH_2$−C−S−$NH_2$ skeletal stretch mode at 733 cm$^{-1}$, and one mode on the low-frequency side of 1093 cm$^{-1}$. In addition, the appearance of very weak peaks at 637 and 653 cm$^{-1}$ has also been observed. There are considerable changes in the spectra in the N−H stretching region too; in particular, all the modes show considerable narrowing and there are two new modes in phase VI as compared to the spectra in phase V. X-ray results indicate considerable changes in the hydrogen-bonding network in phase VI and one hydrogen bond in phase V no longer remains a hydrogen bond in phase VI due to an increase in the N−H···S distance beyond 3.604 A°. We do not observe any major changes in the N−H stretch frequencies except for the fact that the mode at 3232 cm$^{-1}$ sharpens considerably while the one at 3309 cm$^{-1}$ practically disappears. We further observe the appearance of a shoulder on the high-frequency side of the 3177 cm$^{-1}$ mode as can be seen from Figure 2. The splitting and appearance of many new modes in phase VI suggest that the V−VI transition is accompanied by either symmetry lowering or increase in the number of molecules in the unit cell. This agrees with the high-pressure X-ray diffraction study[18] which suggested tripling of the unit cell along the *c*-axis with $Z = 12$,[18] but the observed modes in the Raman spectra are far less than the number expected. The change in the frequencies of the internal modes with increasing pressure is shown in Figure 4, and one observes considerable change in the slopes in most of the modes. In particular, the mode at 1093 cm$^{-1}$ increases at

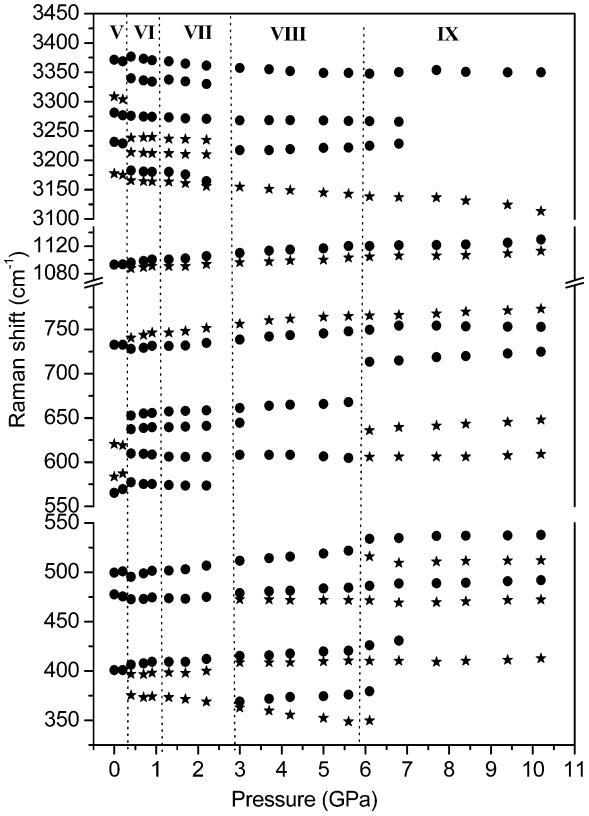


**Figure 4.** Change in frequency of vibrational modes of thiourea over 400−1700 cm$^{-1}$ and 3000−3500 cm$^{-1}$ as a function of pressure.

the rate of 1.5 cm$^{-1}$/GPa till 0.4 GPa, and beyond that it increases rapidly at the rate of 9 cm$^{-1}$/GPa. Also, for the 733 cm$^{-1}$ mode, no slope change is observed till 0.4 GPa and then the two components increase at the rate of 12 and 7 cm$^{-1}$/GPa as shown in Table 2. Thus, the absence of any changes in the internal modes implies negligible deformation of the thiourea molecules, but the translation and rotation of the molecules (as suggested by XRD results) can affect the low-frequency lattice modes as well as the N−H stretch frequencies through the N−H···S hydrogen bonding. A small, but finite, negative slope (Table 3) indicates increasing strength of hydrogen bonding.

**Phase VI−VII.** As the pressure is increased in phase VI, we observe significant changes in the lattice mode region in the spectrum, but not in the mid- and high-frequency region. There is a sudden blue-shift of the two high-frequency modes in the lattice mode region for pressures ≥1 GPa accompanied by a change in the slope of the modes at ≈79, 86, 119, and 138 cm$^{-1}$ as can be seen from Figure 3. The slopes of all the modes decrease considerably, and their values in phases VI and VII are given in Table 1. These changes occurring at ≈1 GPa indicate that the crystal undergoes a phase transition from phase VI to phase VII (say) beyond this pressure. We observe the appearance of a shoulder at 62 cm$^{-1}$ on the high-frequency side of the mode at 57 cm$^{-1}$ for spectra at 1 and 1.6 GPa, and the 57 cm$^{-1}$ mode eventually disappears at 2.4 GPa. It is difficult to understand the origin of this shoulder except for the possibility of coexistence of two phases (VI and VII) at these pressures. The lower-frequency component seems to belong to phase VI, while the higher-frequency component eventually corresponds to phase VII. We do not observe any splitting of modes; however, several internal modes in the mid- and high-frequency region do show change in slopes. Since the changes observed are mainly in the external mode region without the appearance

of any new internal modes, we suggest the possibility of an isostructural phase change across ≈1 GPa from VI to VII.

**Phase VII−VIII.** As the pressure is raised further, we observe gradual changes in the spectrum, and the C−N bending mode at 478 $cm^{-1}$ splits into two modes at ≈3 GPa. Apart from these, new weak peaks appear at 375 and 397 $cm^{-1}$, and the two modes at the ≈1096 $cm^{-1}$ peak get well resolved beyond 3 GPa. These changes are accompanied by a discontinuous change in slope for various modes as shown in Tables 1−3; in particular, the slope of the 141 $cm^{-1}$ mode increases considerably from 4.4 to 13 $cm^{-1}$/GPa beyond 3 GPa as can be seen in Figure 3. The observed discontinuity in slope and the splitting of the existing Raman modes accompanied by emergence of new Raman modes at ≈3 GPa suggest another transition from VII to VIII phase (say) and the new phase is of lower symmetry. A possible space group of lower symmetry is $D_2$ where the mirror plane of $D_{2h}$ is missing, and here each of the $A'$ and $A''$ symmetry of the site group goes over to two Raman active modes resulting in the splitting of the modes.

**Phase VIII−IX.** On further increase in pressure in phase VIII, the spectra undergo gradual changes and a sudden change is observed beyond ≈6.1 GPa. For example the lowest-frequency lattice mode at ≈68 $cm^{-1}$ rapidly decreases in intensity and vanishes by 7 GPa. There is considerable intensity redistribution among three modes at ≈166 $cm^{-1}$, and the lowest-frequency mode gains in intensity at the expense of the other two. We also observe several changes in the mid- as well as high-frequency region. The $NH_2$ twist mode at 500 $cm^{-1}$ splits into two components, and three new modes appear at ≈606, 636, and 713 $cm^{-1}$. The mode at 636 $cm^{-1}$ is very weak, and the one at 713 $cm^{-1}$ appears as a broad shoulder. The in-plane $NH_2-CS-NH_2$ bending modes at 733 $cm^{-1}$ undergo drastic changes with complete reversal of the intensity of the two modes, and the lower-frequency component gradually merges with the higher-frequency component. In the high-frequency N−H stretching region, the spectra show sudden changes beginning at ≈6.1 GPa. All these changes indicate another transition from phase VIII to a new phase IX (say) at ≈6.1 GPa.

As the pressure is increased in phase IX all the modes start broadening and by 10.5 GPa, the lines become very broad and weak in intensity. We did not follow the spectral changes beyond this pressure. The variation in the low-frequency modes with increasing pressure is shown in Figure 3 up to the pressure of 7.7 GPa, as it had become difficult to obtain the exact peak positions due to the large broadening of the modes beyond this pressure. However, many of the modes in the mid- and high-frequency region could be followed till the highest pressure, and the changes observed in the N−H stretching region are most interesting. The modes at ≈3225 and 3267 $cm^{-1}$ broaden to such an extent that they cannot be followed beyond ≈7 GPa, while the mode at 3372 $cm^{-1}$ remains sharp and quite intense till the highest pressure. The sharp nature and negligible change in the frequency of the 3372 $cm^{-1}$ mode indicate that the strength of the hydrogen bond reaches saturation even with an increase in pressure.

We have thus observed that thiourea undergoes a series of transitions as the pressure is increased up to ≈11 GPa, and all of these have been found to be completely reversible. This reversibility suggests that there is no permanent change in the molecular arrangement and their interaction in all the high-pressure phases. Our Raman scattering results can thus be be summarized as follows:

$$\text{Phase V} \xrightarrow{\approx 0.35\ \text{GPa}} \text{VI} \xrightarrow{\approx 1\ \text{GPa}} \text{VII} \xrightarrow{\approx 3\ \text{GPa}} \text{VIII} \xleftarrow{\approx 6.1\ \text{GPa}} \text{IX}$$

## 4. Conclusion

Our high-pressure phase transitions in thiourea till ≈11 GPa using Raman spectroscopy suggest the existence of four phase transitions at ≈1, 3, and 6.1 GPa, in addition to the transition observed earlier at 0.35 GPa. The emergence of several new modes, splitting of existing modes, changes in slope of the frequency−pressure curve for several modes, and intensity redistribution indicates lowering of symmetry across these transitions. We further emphasize that these transitions are completely reversible. Our results can be compared with the high-pressure study carried out in the analogous compound (urea) which also reports the existence of four transitions till 12 GPa. The high-pressure phases for urea have been identified to be of lower symmetry using in situ XRD studies, and this agrees with our suggestion in thiourea of the transition to phases of lower symmetry at high pressure.

## References and Notes

(1) Leonidva. G. G. *Fiz. Tverd. Tela* **1963**, 5, 3430 (translation: *Sov. Phys. Solid State* **1964**, *5*, 2519).
(2) Gesi, K. *J. Phys. Soc. Jpn*. **1969**, *26*, 107.
(3) Klimowski, J.; Wanarski, W.; Ozgo, D. *Phys. Status Solidi A* **1976**, *34*, 697.
(4) Calvo, C. *J. Chem. Phys*. **1960**, *33*, 1721, and references therein.
(5) Denoyer, F.; Currat, R. *Incommensurate Phases in Dielectric*; Blinc, R., Levanyuk, A. P., Eds.; Elsevier: New York, 1986; Vol. 2, p 129.
(6) Pillai, K. C.; Narayan, R. *J. Electrochem. Soc*. **1978**, *125*, 1393.
(7) Dayalan, E.; Narayan, R. *J. Electroanal. Chem*. **1984**, *179*, 167.
(8) Soute, R. M.; Gonzales, S.; Arevale, A. *J. Electroanal. Chem*. **1987**, *216*, 273.
(9) Truter, M. R. *Acta Crystallogr*. **1967**, *22*, 556.
(10) Masunov, A.; Dannenberg, J. J. *J. Phys. Chem. B* **2000**, *104*, 806.
(11) Goldsmith, G. J.; White, J. G. *J. Chem. Phys*. **1959**, *31*, 1175.
(12) Elcombe, M.; Taylor, J. C. *Acta Crystallogr*. **1968**, *A24*, 410.
(13) Bandy, A.; Cessac, G. L.; Lippincott, E. R. *Spectrochim. Acta* **1972**, *28A*, 807, and references therein.
(14) Bridgman, P. W. *Proc. Am. Acad. Art. Sci*. **1937**, *72*, 227.
(15) Figuiere, P.; Ghelfenstein, M.; Szwarc, H. *Chem. Phys. Lett*. **1975**, *33*, 99.
(16) Leonidova, G. G. *Fiz. Tverd. Tela* **1963**, *5*, 3430.
(17) Kabalkina, S. S. *Zh. Fiz. Khim*. **1961**, *35*, 276.
(18) Asahi, T.; Hasebe, K.; Onodera, A. *J. Phys. Soc. Jpn*. **2000**, *69*, 2895.
(19) Karmakar, S.; Sharma, S. M. *Solid State Phys*. **2003**, *46*, 55.
(20) Lamelas, F. J.; Dreger, Z. A.; Gupta, Y. M. *J. Phys. Chem. B* **2005**, *109*, 8206.
(21) Sharma, S. M.; Gupta, Y. M. *Phys. Rev*. **1991**, *B43*, 879.
(22) Schrader, B.; Meier, W.; Takahashi, H. *Ber. Bunsen-Ges*. **1971**, *75*, 1263.
(23) Vijay, A.; Sathyanarayana, D. N. *Spectrochim. Acta* **1993**, *49A*, 1565.
(24) Bencivenni, L.; Nunziante Cesaro, S. *Vib. Spectrosc*. **1998**, *18*, 91.
(25) Iqbal, Z.; Christoe, C. W. *Chem. Phys. Lett*. **1976**, *37*, 460.